



A family of hydroxypyronone ligands designed and synthesized as iron chelators

Leonardo Toso^a, Guido Crisponi^{a,*}, Valeria M. Nurchi^a, Miriam Crespo-Alonso^a, Joanna I. Lachowicz^a, M. Amelia Santos^b, Sergio M. Marques^b, Juan Niclós-Gutiérrez^c, Josefa M. González-Pérez^c, Alicia Domínguez-Martín^c, Duane Choquesillo-Lazarte^d, Zbigniew Szewczuk^e

^a Dipartimento di Scienze Chimiche e Geologiche, Università di Cagliari, Cittadella Universitaria, 09042 Monserrato Cagliari, Italy

^b Centro Química Estrutural, Instituto Superior Técnico, Universidade Técnica de Lisboa, Av. Rovisco Pais, 1049-001 Lisboa, Portugal

^c Department of Inorganic Chemistry, Faculty of Pharmacy, Campus Cartuja, University of Granada, E-18071 Granada, Spain

^d Laboratorio de Estudios Cristalográficos, IACT, CSIC-Universidad de Granada, Av. de las Palmeras 4, E-18100 Armilla, Granada, Spain

^e Faculty of Chemistry, University of Wrocław, F. Joliot-Curie 14, 50-383 Wrocław, Poland

ARTICLE INFO

Article history:

Received 26 December 2012

Received in revised form 15 June 2013

Accepted 17 June 2013

Available online 26 June 2013

Keywords:

Kojic acid

Fe^{III}

Solution equilibria

X-Ray structure

Synthesis

Hydroxypyrones

ABSTRACT

The use of chelating agents for iron and aluminum in different clinical applications has found increasing attention in the last thirty years. Desferal, deferiprone and deferasirox, chelating agents nowadays in use, are based on hydroxamic groups, hydroxyl-substituted pyridinones or aromatic ring systems. With the aim of designing new chelators, we synthesized a series of kojic acid derivatives composed by two kojic units joined by linkers variously substituted. The huge advantages of these molecules are that they are easy and cheap to produce. Preliminary works on complex formation equilibria of the first group of ligands with iron and aluminium highlighted extremely good pMe values and gave evidence of the ability to scavenge iron from inside cells. On these bases a second set of bis-kojic ligands, whose linkers between the kojic chelating moieties are differentiated both in terms of type and size, has been designed, synthesized and characterized. The structural characterization of these new ligands is presented, and the protonation and iron^{III} complex formation equilibria studied by potentiometry, UV–Visible spectrophotometry, electrospray ionization mass (ESI-MS) and ¹H NMR spectroscopy will be described and discussed.

© 2013 Elsevier Inc. All rights reserved.

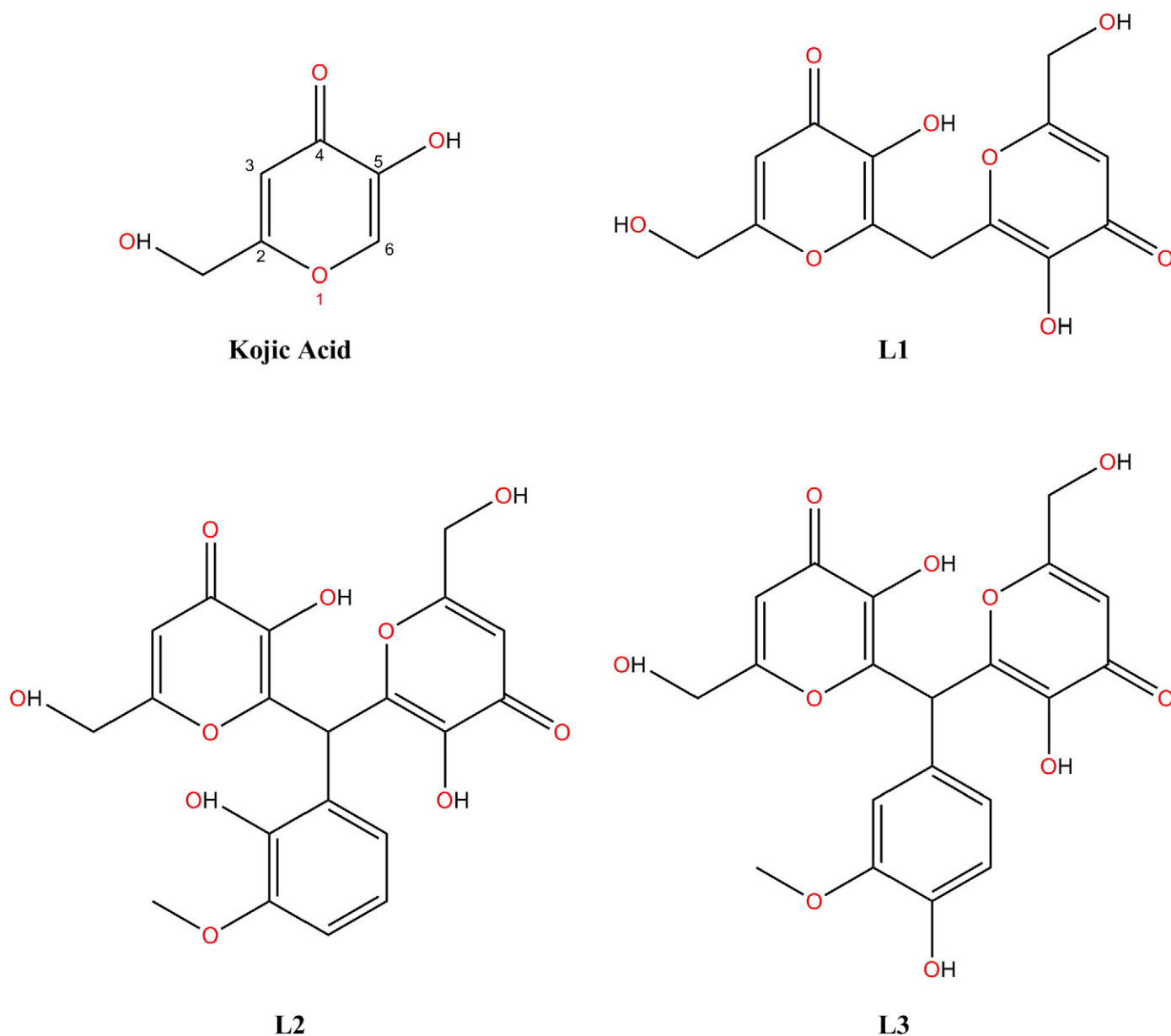
1. Introduction

In the last two decades there has been an increasing interest in the use of chelation therapy for various health diseases depending on iron and aluminium overload [1–6]. Drugs in current use, such as desferal, deferiprone and deferasirox, include 1–3 chelating groups, typically hydroxamic groups, hydroxyl-substituted pyridinones or aromatic ring systems. In the above mentioned reviews the numerous drawbacks limiting in some instance the use of these drugs are presented and discussed, and the need of new effective iron chelators is stressed. With the aim of designing new ligands that form complexes with high stability, selectivity, lipophilicity and bioavailability, which satisfy both the chemical requirements and biological constraints for an effective therapeutic agent, we synthesized some derivatives of kojic acid, and studied their complex formation equilibria with Fe^{III} and Al^{III}, as well as those with the parent ligand kojic acid, 5-hydroxy-2-(hydroxymethyl)-4H-pyran-4-one, (Scheme 1).

In a previous work, evidence was given on the formation of MeL, MeL₂, and MeL₃ complexes of Al^{III} and Fe^{III} with kojic acid, confirmed by the X-ray structure of the FeL₃ complex, and of diverse protonated species of Me₂L₂ and MeL₂ complexes with L1 [7]. On the basis of the extremely good pFe value (23.1) characterizing L1, and of its ability to scavenge iron from inside cells [8], we extended the investigation to the related compounds in which vanillin and ortho-vanillin (L2 and L3) substituents were inserted on the linker joining the two kojic units. Similar complexes to those formed with L2 were found. In the binuclear Me₂L₂ complexes, each metal ion is coordinated by two COC(OH)-chelating moieties, one from each coordinating molecules: actually, the length of the linker between the two kojic units prevents metal ion coordination by both kojic units on the same molecule. The found pFe values (18.9 for L2 and 22.2 for L3), lower than that of desferal (26.6) and comparable with that of deferiprone (20.7), were very encouraging [9,10]. These ligands are easy and cheap to produce, as the starting materials, kojic acid and vanillin, are not expensive. Hence, they are worthy of further tests on their toxicity and their capacity to remove iron and/or aluminium from intra-cellular sites in living organisms. Aimed at improving the interaction between the kojic moieties and the metal ions, we have designed and synthesized a new set of bis-kojic ligands whose linkers (between the two kojic

* Corresponding author at: Dipartimento di Scienze Chimiche e Geologiche, Cittadella Universitaria, 09042 Monserrato, Cagliari, Italy. Tel.: +39 070 675 4476; fax: +39 070 675 4478.

E-mail address: crisponi@unica.it (G. Crisponi).



Scheme 1. Chemical structures and acronyms of studied ligands.

chelating moieties) are differentiated both in terms of type and size (Scheme 2).

In this paper we will report the synthesis of the new derivatives, namely L4, L5, L6, and L7 containing an amine group in the linker and also L8, which is a L1 analog but with insertion of a methyl group in the linker. The acid-base properties, together with the equilibrium constants for the formation of Fe^{III} complexes as well as the structure characterization of L6, L7 and L8 by X-Ray diffraction will be presented herein.

2. Experimental

2.1. Reagents

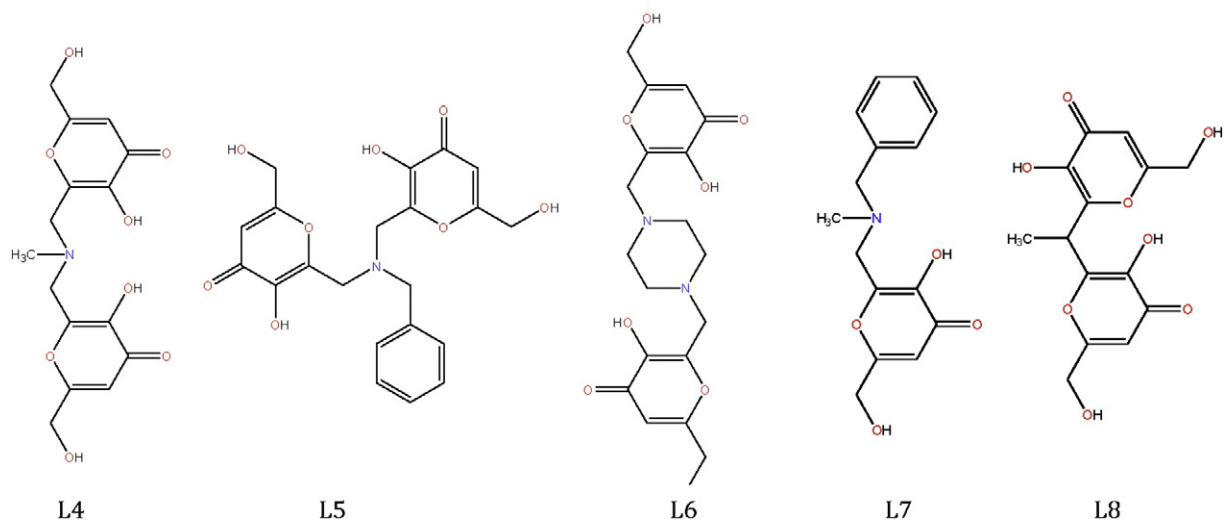
Kojic acid, benzylamine hydrochloride, piperazine, methylamine hydrochloride, NaOH, KOH, FeCl_3 , methanol, ethanol and 2-isopropanol were purchased from Aldrich, and N-benzylmethylamine was an Alfa Aesar product. Formaldehyde was purchased from Merck, HCl from Fluka, and KCl and ZnO from Carlo Erba (Milan, Italy). Desferal was a

Biofutura Pharma product. All the products were used without any further purification.

A previous described method was used in the preparation of 0.1 M carbonate free KOH solution [11]. Ligand solutions were acidified with stoichiometric equivalents of HCl. Fe^{III} solution was prepared by dissolving the required amount of FeCl_3 in pure double distilled water to which a stoichiometric amount of HCl was previously added to prevent hydrolysis. This solution was standardized by spectrophotometric titration with desferal.

2.2. Synthesis

All the ligands were prepared from 6-alkylation of kojic acid (KA) with an aldehyde and a primary amine or an inorganic base, depending on desired presence or absence of amine group on that alkyl substituent. The particular operations are reported in the following for each single ligand. For each ligand preparation, a KA (1.00 g, 7.1 mmol) solution in ethanol (25 mL) was used. All the reactions were followed by TLC, using a CH_2Cl_2 :MeOH (12:1) mixture as eluent. The synthesized products



Scheme 2. Chemical structures and acronyms of studied ligands.

were fully characterized by different standard instrumental techniques. NMR spectra were recorded on a Bruker AVANCE III spectrometer at 300 MHz and 400 MHz for ^1H NMR and ^{13}C NMR respectively. Chemical shifts (δ) are reported in ppm related to tetramethylsilane (TMS). Infrared spectra were recorded by using KBr pellets on a Jasco FT-IR 410 spectrometer. The electrospray ionization mass spectra (ESI-MS) were obtained on a 500 MS LC Ion Trap (Varian Inc., Palo Alto, CA, USA) mass spectrometer equipped with an ESI ion source, operated in the positive and negative ion modes. The elemental analyses were performed on a Fisons EA1108 CHNS-O within the limit of $\pm 0.4\%$. Although some of the compounds gave unsatisfactory analysis values, for which found values differ by more than $\pm 0.5\%$ from Calc. values, crystal structures of all of these compounds were determined by X-ray diffraction (XRD) technique or their structures were supported by spectroscopic (FT-IR, ^{13}C -NMR and ESI-MS) analyses.

2.2.1. 6,6'-(Methylazanediyloxy)bis(methylene)bis(5-hydroxy-2-(hydroxymethyl)-4H-pyran-4-one), L4

Methylamine hydrochloride (0.260 g, 3.8 mmol), previously neutralized with NaOH (3.8 mmol), was added to a solution containing formaldehyde (580 μL , 7.1 mmol) in ethanol (2 mL). The mixture was stirred for 30 min at room temperature, then added drop wise to the kojic ethanolic solution described above. The solution was left under stirring for 1.5 h in a water bath at 40/50 $^\circ\text{C}$. Solvent was removed under vacuum. Addition of CH_3CN yielded a white precipitate that was filtered off, washed with cold CH_3CN , and dried under vacuum for 6 h. Recrystallization afforded the pure product as a white solid (1.09 g, 92% yield). Mp = 150–152 $^\circ\text{C}$. Elemental analysis found (calc. for $\text{C}_{15}\text{H}_{17}\text{NO}_8$): C, 52.76 (53.10); H, 5.48 (5.05);

N, 4.20 (4.13). FT-IR (KBr, 4000–400 cm^{-1}): $\nu_{\text{as}}(\text{CH}_3)$ 2963, $\nu_{\text{as}}(\text{CH}_2)$ 2923, $\nu_{\text{d}}(\text{CH}_3)$ 2888, $\nu_{\text{s}}(\text{CH}_2)$ 2853, $\nu(\text{C}=\text{O})$ 1665, $\delta(\text{CH}_2)$ 1460, $\nu(\text{C}-\text{O}-\text{C})_{\text{cyclic}}$ 1218, $\pi(\text{C}-\text{H})_{\text{ar}}$ (kojic) 854. ^1H -NMR (400 MHz, MeOD): δ 6.380(2H, s), 4.350(4H, s), 3.763(4H, s), 2.403(3H, s). ^{13}C -NMR (400 MHz, MeOD): δ 145.30 (C), 148.03 (C), 169.86 (C), 179.95 (C), 110.09 (CH), 43.11 (CH_2), 54.37 (CH_2), 61.23 (CH_2). ESI-MS(-): MH^- (338.2), $[\text{M} + \text{Cl}]^-$ (374.2).

2.2.2. 6,6'-(Benzylazanediyloxy)bis(methylene)bis(5-hydroxy-2-(hydroxymethyl)-4H-pyran-4-one), L5

Benzylamine hydrochloride (0.51 g, 3.5 mmol), previously neutralized with NaOH (3.5 mmol), was added to a solution of formaldehyde (633 μL , 7.8 mmol) in ethanol (2 mL). The mixture was stirred for 30 min at room temperature and then added drop wise to the kojic

ethanolic solution. The solution was left under stirring for 3.5 h in a water bath at 40/50 $^\circ\text{C}$. Solvent was removed under vacuum. Red impurities were removed from the white precipitate by several double distilled cold water washings, filtrations and dryings under vacuum. Recrystallization yielded the pure final product (0.84 g, 57%). Mp = 126–128 $^\circ\text{C}$. Elemental analysis found (calc. for $\text{C}_{21}\text{H}_{21}\text{NO}_8$): C, 59.43 (60.72); H, 5.58 (5.10); N, 3.42 (3.37). FT-IR (KBr, 4000–400 cm^{-1}): two types of $\nu_{\text{as}}(\text{CH}_2)$ 2960 and 2925, two types of $\nu_{\text{s}}(\text{CH}_2)$ 2888 and 2851, $\nu(\text{C}=\text{O})$ 1644, $\delta(\text{CH}_2)$ 1454, $\nu(\text{C}-\text{N})_{\text{tertiary amine}}$ 1360, $\nu(\text{C}-\text{O}-\text{C})_{\text{cyclic}}$ 1223, $\pi(\text{C}-\text{H})_{\text{ar}}$ (kojic) 858, $\pi(\text{C}-\text{H})_{\text{ar}}$ (benzyl) 747 and 701. ^1H -NMR (300 MHz, MeOD): δ 7.203(5H, Ph), 6.295(2H, S), 4.306(4H, s), 3.792(4H, s), 3.751(2H, s). ^{13}C -NMR (300 MHz, MeOD): δ 139.10(C), 144.86(C), 149.24(C), 169.68(C), 176.27(C), 109.97(CH), 128.59(CH), 129.32(CH), 130.16(CH), 52.26(CH_2), 60.44(CH_2), 61.21(CH_2). ESI-MS(-): MH^- (414.2), $[\text{M} + \text{Cl}]^-$ (450.2).

2.2.3. 6,6'-(Piperazine-1,4-diylbis(methylene))bis(5-hydroxy-2-(hydroxymethyl)-4H-pyran-4-one), L6

Piperazine (0.305 g, 3.5 mmol) was added to a solution of formaldehyde (580 μL , 7.1 mmol) in ethanol (2 mL). The mixture was stirred for 30 min at room temperature and then added drop wise to a kojic ethanolic solution. The solution was left under stirring for 5 h during which a fine white precipitate appeared. Upon refrigeration for 2 h, the reaction mixture was filtered off, washed with cold ethanol and dried under vacuum for 6 h. Recrystallization afforded the final product 1.35 g, 97%). Mp > 350 $^\circ\text{C}$. Elemental analysis found (calc. for $\text{C}_{18}\text{H}_{22}\text{N}_2\text{O}_8$): C, 54.18 (54.82); H, 6.07 (5.62); N, 7.17 (7.10). FT-IR (KBr, 4000–400 cm^{-1}): two types of $\nu_{\text{as}}(\text{CH}_2)$ 2951 and 2917, two types of $\nu_{\text{s}}(\text{CH}_2)$ 2880 and 2839, $\nu(\text{C}=\text{O})$ 1653, $\delta(\text{CH}_2)$ 1460, $\nu(\text{C}-\text{O}-\text{C})_{\text{cyclic}}$ 1244, $\pi(\text{C}-\text{H})_{\text{ar}}$ (kojic) 867, $\pi(\text{C}-\text{H})_{\text{ar}}$ (piperazine) 824. ^1H -NMR (300 MHz, MeOD + KOD): δ 6.120(2H, S), 4.179(4H, s), 3.530(4H, s), 2.490(8H, s). ^{13}C -NMR (400 MHz, MeOD + KOD): δ 148.782 (C), 154.936 (C), 165.674 (C), 183.262 (C), 109.646 (CH), 53.455 (CH_2), 55.127 (CH_2), 61.801 (CH_2). ESI-MS(-): MH^- (393.3).

2.2.3.1. Synthesis of L6 crystal. L6 (15 mg) was dissolved in distilled water (12 mL), aided by drop wise addition of HCl 0.01 M. Afterwards, isopropanol (4 mL) was added and the solution was left stirring for 30 min and then filtered into a crystallization device to remove possible impurities. The solution was left stand at room temperature in order to evaporate. Evaporation of the solvents was controlled with the aid of a plastic film. After three weeks, parallelepiped colorless crystals appeared suitable for XRD.

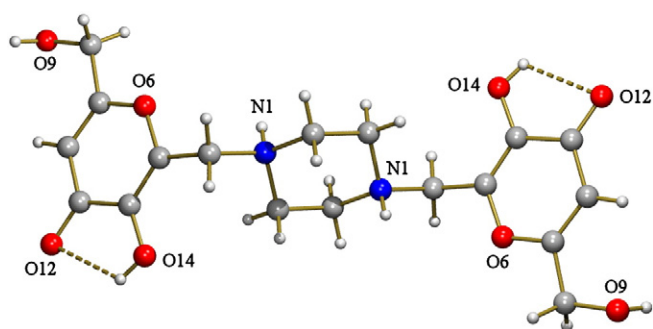


Fig. 1. Centro-symmetrical H_2L6^{2+} ion in the crystal of ligand L6. Intra-molecular H-bonding interactions are depicted in dotted lines.

2.2.4. 2-((Benzyl(methyl)amino)methyl)-3-hydroxy-6-(hydroxymethyl)-4H-pyran-4-one, L7

N-Benzylmethylamine (967 μ L, 7.8 mmol) was added to a solution of formaldehyde (633 μ L, 7.8 mmol) in ethanol (2 mL). The mixture was stirred for 30 min at room temperature and then added drop wise to the kojic ethanolic solution described above. The solution was left under stirring for 5 h. Solvent was removed under vacuum until a white precipitate was formed. Upon refrigeration for 2 h it was filtered off washed with cold ethanol and dried under vacuum for 6 h. Recrystallization afforded the final pure product (1.69 g, 87%). Mp = 137–139 °C. Elemental analysis found (calc. for $C_{15}H_{17}NO_4$): C, 65.12 (65.44); H, 6.14 (6.22); N, 5.11 (5.09). FT-IR (KBr, 4000–400 cm^{-1}) $\nu_{as}(CH_3)$ 2989, two types of $\nu_{as}(CH_2)$ 2951 and 2938, $\nu_d(CH_3)$ 2884, $\nu_s(CH_2)$ 2831, $\nu(C=O)$ 1662, $\delta(CH_3)$ 1496, $\delta(CH_2)$ 1465, $\nu(C-N)_{tertiary\ amine}$ 1360, $\nu(C-O-C)_{cyclic}$ 1244, $\pi(C-H)_{ar}$ (kojic) 853, $\pi(C-H)_{ar}$ (benzyl) 747 and 701. ^1H-NMR (300 MHz, $D_2O + KOD$, pH = 12): δ 7.351(5H, Ph), 6.331(1H, S), 4.417(2H, s), 3.684(2H, s), 3.601(2H, s), 2.249(3H, s).

2.2.4.1. Synthesis of L7 crystal. L7 (30 mg) was dissolved in a $H_2O/MeOH$ (1:1) mixture (16 mL). After 30 min stirring, a clear colorless solution was obtained. The solution was filtered into a crystallization device and covered with a plastic film to control the evaporation of the solvents. In one week, parallelepiped colorless crystals were collected for XRD analysis.

2.2.5. 2-2'-Ethanediylbis(3-hydroxy-6-(hydroxymethyl)-4H-pyran-4-one), L8

Synthesis of L8 was carried out according to literature methods [12]. 6.2 g of kojic acid and an equivalent amount of aldehyde were dissolved in (100 mL) ethanol. The reaction, catalyzed by of concentrated ammonium hydroxide (1 mL), was heated for three hours at 60 °C. Then the solvent was left to evaporate and the beige precipitate was washed with cold ethyl alcohol. Recrystallization from ethanol yield

the pure final product (4.61 g, 68%). Mp = 207–208 °C. Elemental analysis found (calc. for $C_{14}H_{14}O_8$): C, 54.20 (55.70); H, 5.03 (4.55). FT-IR (KBr, 4000–400 cm^{-1}) $\nu_{as}(CH_3)$ 2983, $\nu_{as}(CH_2)$ 2940, $\nu_d(CH_3)$ 2879, $\nu_s(CH_2)$ 2850, $\nu(C=O)$ 1653, $\delta(CH_2)$ 1463, $\nu(C-O-C)_{cyclic}$ 1265, $\pi(C-H)_{ar}$ (kojic) 857. ^1H-NMR (300 MHz, $D_2O + KOD$, pH = 6): 6.560(2H, s), 4.530 (4H, s), 1.660 (3H, d).

2.2.5.1. Synthesis of L8 crystal. L8 (10 mg) was dissolved in EtOH (10 mL) under moderate heating (35 °C) and stirred until a clear colorless solution was obtained. Afterwards, the solution was filtered into a crystallization device and covered with a plastic film to control the evaporation of the solvent. In one week, small parallelepiped colorless crystals appeared. In order to improve the size of the crystals, successive filtrations of the mother liquors were performed until suitable crystals for XRD purposes were collected.

2.3. Potentiometric–Spectrophotometric measurements

Protonation and complex-formation equilibrium studies were carried out under the same conditions described in a previous publication [7]. The operating ligand concentrations ranged from 3×10^{-4} to 3×10^{-3} M according to the examined ligand. The studies of complex formation were carried using constant ligand concentration, and 1:1, 1:2, and 1:3 metal/ligand molar ratios. Combined potentiometric–spectrophotometric measurements were performed for protonation equilibria in the 200–400 nm spectral range and in the 400–800 nm spectral range for Fe^{III} complexes, using 0.2 and 1 cm path lengths. Protonation and complex formation data were analyzed using the Hyperquad program [13].

2.4. ESI-MS analysis of complexes

ESI-MS spectra were carried out on a Bruker microTOF-Q spectrometer (Bruker Daltonik, Bremen, Germany) equipped with an ESI source. Samples were dissolved in water and methanol (molar ratio 1:1) and the final pH was ~ 7 . The ligand concentration was $\sim 10^{-5}$ M and the ligand to metal molar ratio was 1:10. The experiment parameters were as follows: scan range: m/z 100–1600; drying gas: nitrogen; and temperature: 200 °C, ion source voltage 4500 V, collision energy 10 eV. The instrument was operating in the positive ion mode and calibrated externally with Tunemix™ mixture (Bruker Daltonik, Germany). Analyte solutions were inserted at a flow rate of 3 μ L/min. Compass Data Analysis (Bruker Daltonik, Germany) program was used to determine the formulae of the complexes. The distance between peaks allowed calculating the charge of the analyzed ions. In the MS/MS experiments, the ion corresponding to signal at m/z 392 was selected on the quadrupole and subsequently fragmented in the collision cell. Argon was used as a collision gas. The obtained fragments were directed to the mass

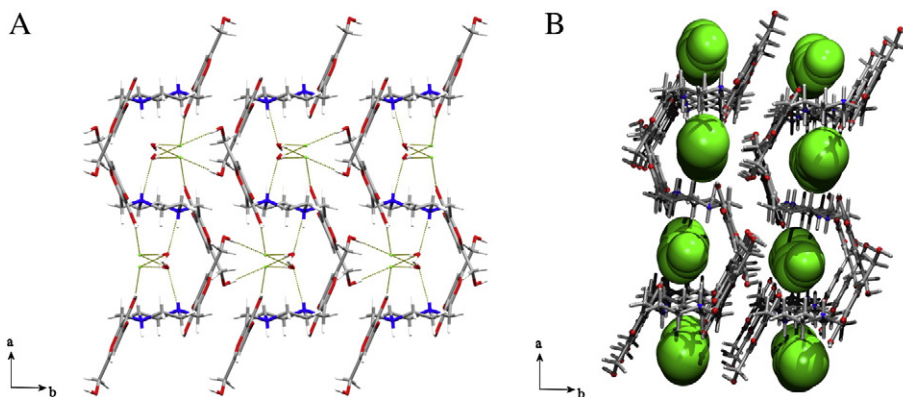


Fig. 2. View in the ab plane of the H-bonded 3D network of the crystal of L6. A) Chloride ions and water molecules are hosted in the corresponding channels throughout the c axis. B) Chloride ions and water molecules are removed and the total accessible voids are plotted in green space fill.

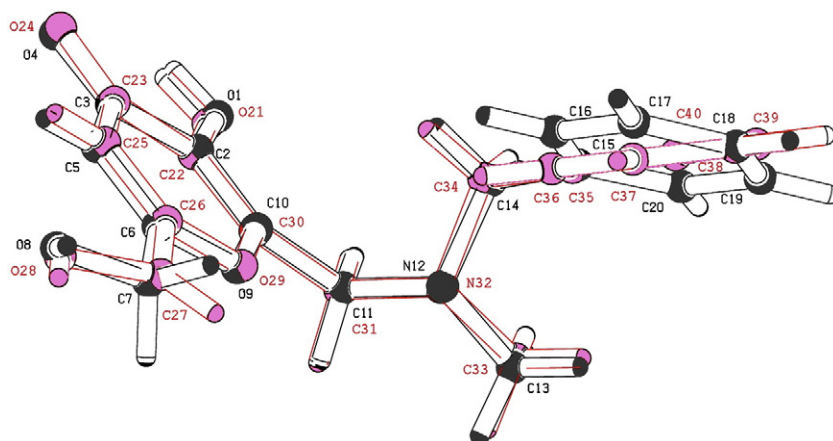


Fig. 3. Overlapped view of the two non-equivalent molecules within the asymmetric unit in the crystal of ligand L7. Molecule 1 is depicted in darker line whereas molecule 2 is depicted in lighter line. Numbering scheme is also provided. Intra-molecular H-bonding interactions are omitted for clarity.

analyzer and registered as an MS/MS spectrum. The collision energy was 10 eV.

2.5. Crystal structure determination

Measured crystals L6, L7 and L8 were prepared under inert conditions immersed in perfluoropolyether as protecting oil for manipulation. Suitable crystals were mounted on MiTeGen Micromounts™ and these samples were used for data collection. Data were collected with Bruker SMART APEX [L6 (293 K), L7 (296 K) and L8 (100 K)] diffractometer. The data were processed with APEX2 [14] program and corrected for absorption using SADABS [15]. The structures were solved by direct methods, which revealed the position of all non-hydrogen atoms. These atoms were refined on F^2 by a full-matrix least-squares procedure using anisotropic displacement parameters [16]. All hydrogen atoms were located in difference Fourier maps and included as fixed contributions riding on attached atoms with isotropic thermal displacement parameters 1.2 times those of the respective atom. Geometric calculations were carried out with PLATON [17] and drawings were produced with PLATON and MERCURY [18]. Additional crystal data and more information about the X-ray structural analyses are shown in Supplementary material S1 to S3. Crystallographic data for the structural analysis have been deposited with the Cambridge Crystallographic Data Centre, CCDC 914446–914448 from L6 to L8, respectively. Copies of this information may be obtained free of charge on application to CCDC, 12 Union Road, Cambridge CB2 1EZ, UK (fax: 44 1223 336 033; e-mail: deposit@ccdc.cam.ac.uk or <http://www.ccdc.cam.ac.uk>).

In addition, one red parallelepiped crystal obtained from the synthesis of one Fe/L6 complex was mounted on a MiTeGen Micromount™ and this sample was used for data collection. Data was collected at the ESRF synchrotron ID14-1 beamline ($\lambda = 0.9340 \text{ \AA}$, 100 K). Previous attempts to determine the structure of these iron compound using conventional X-ray diffraction facilities were unsuccessful provided the poor diffraction power of the crystal samples. Only a tentative model for the iron(III) compound $\text{Fe}_2(\text{L6})_3$ can be proposed due to the limited resolution achieved in the experiment. Constraints were used to model the aromatic rings and the piperazine moiety of L6 ligand. The diffuse scattering contribution from solvent and data noise was removed using the SQUEEZE procedure in PLATON [17].

3. Results and discussion

3.1. Crystal structure of ligands L6, L7, L8

3.1.1. Crystal structure of the ligand L6: $(\text{H}_2\text{L6})\text{Cl}_2 \cdot 2\text{H}_2\text{O}$

The crystal of ligand L6 (monoclinic system, space group $P2_1/c$) consists of one dichlorhydrate acid molecule and two water molecules. Note that an inversion center is located in the middle of the acid molecule, thus L6 is centro-symmetric (Fig. 1).

The molecule shows the most stable trans-e, e-conformation. The kojic acid moieties are stabilized by two intra-molecular H-bonds involving the OH phenol-like groups as donors and the O keto-kojic groups as acceptors [O14–H···O12 (2.742(2) Å, 113.3°)]. This latter feature has also been observed in closely related kojic-like compounds [9].

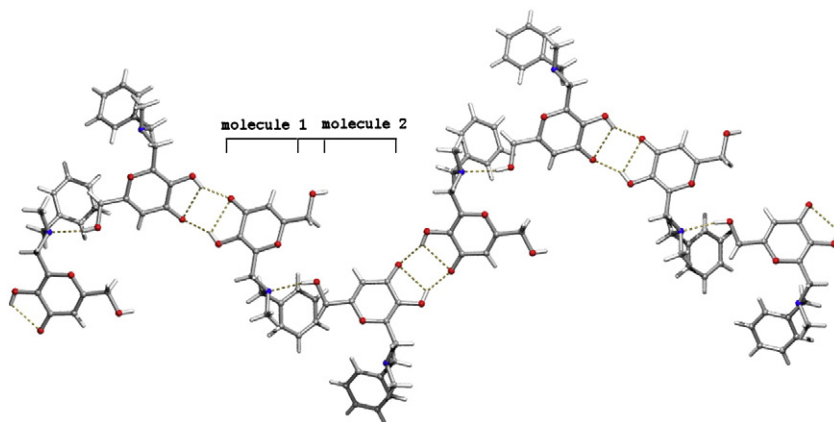


Fig. 4. Fragment of one zig-zag 1D chain in the crystal of ligand L7. Note that the OH phenol-like group is involved in a bifurcated interaction acting as H-donors for one intra- and one inter-molecular interactions. Likewise, the O keto-kojic group also acts as double H-acceptor from one intra- and one inter-molecular interactions.

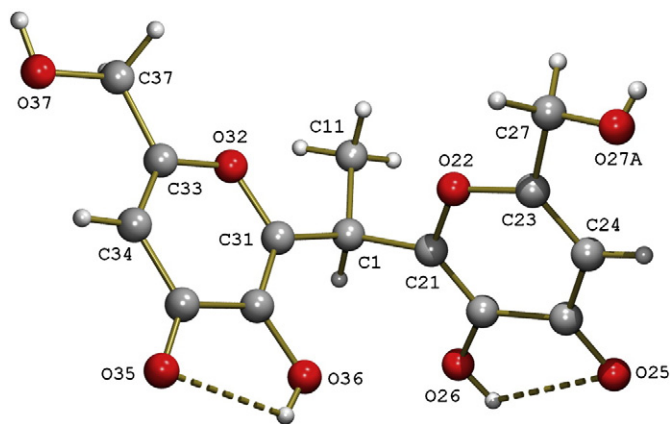


Fig. 5. Asymmetric unit in the crystal of ligand L8. Intra-molecular H-bonding interactions are plotted. Only one of the disordered positions of the hydroxyl-methyl arm is depicted for clarity.

Table 1

Protonation constants of the ligands at 25 °C, 0.1 M KCl ionic strength, obtained from potentiometric titration curves using the Hyperquad program [13].

	L4	L5	L6	L7	L8
logK ₁	9.19(3)	9.01(2)	8.52(4)	8.49(1)	9.49(3)
logK ₂	7.51(3)	7.61(2)	7.81(2)	6.02(2)	6.69(5)
logK ₃	4.38(5)	3.35(2)	5.49(5)	–	–
logK ₄	–	–	1.97(5)	–	–

The crystal of L6 is a 3D network built thanks to the involvement of H₂O and H₂L6²⁺ and Cl[−] ions in H-bonding interactions (see Table S1.3). In particular, chloride ions and water molecules are located in cavities that extend along the *c* axis and kept inside due to hydrogen bonding interactions involving all the donors from L6 acid molecule. The total accessible void calculated by PLATON [17] is found to be 18.8% of the crystal volume (Fig. 2).

3.1.2. Crystal structure of the ligand L7: (L7)₂

Ligand L7 crystallizes in the monoclinic system, space group P2₁/c. The asymmetric unit of the crystal comprises two crystallographically independent molecules of ligand L7. The reason why the two former

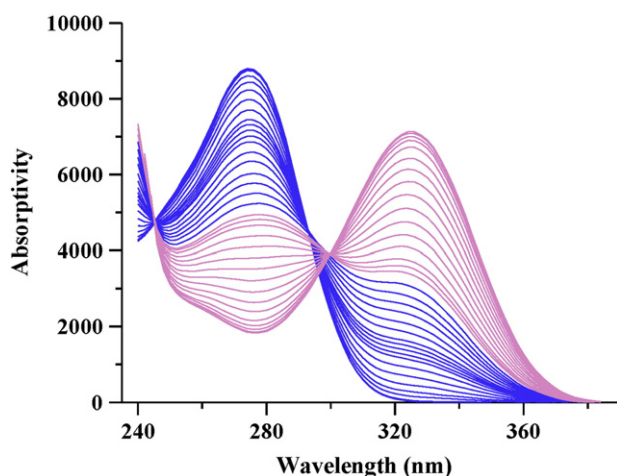


Fig. 6. Spectra collected during the potentiometric titration of ligand L7. Blue (darker lines) spectra are collected in the pH range relative to the first deprotonation, pink (lighter lines) spectra in the pH range relative to the second deprotonation.

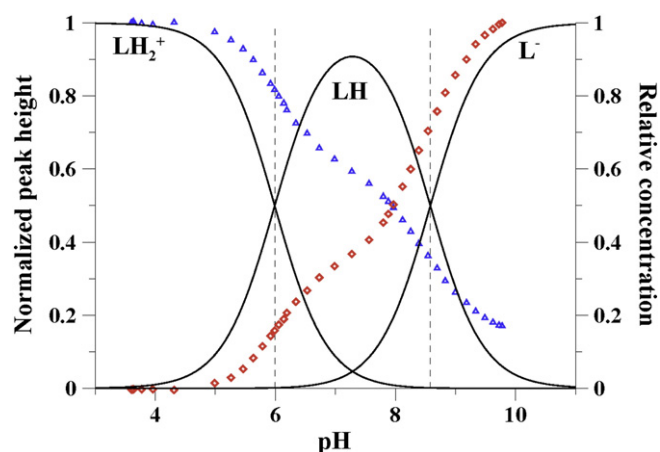


Fig. 7. Speciation curves of ligand L7, with the overlapping trends of the heights of UV bands at 276 nm (Δ) and 322 nm (\diamond), obtained by spectral decomposition of the spectra in Fig. 6 with the Specpeak program (19).

molecules are not equivalent mainly deals with the different torsion angles defined by the benzyl moiety [molecule 1: <N12–C14–C15–C16 85.78° or molecule 2: <N32–C34–C35–C36 108.05°] (see Fig. 3).

As already described for compound L6, each L7 molecule exhibits one intra-molecular H-bond that, again, involve the OH phenol-like group as donor and the O keto-kojic group as acceptor [molecule 1: O1–H··O4 (2.757(2) Å, 112.8°) or molecule 2: O21–H··O24 (2.764(2) Å, 112.6°)]. Moreover, the independent two molecules within the asymmetric unit are associated by one inter-molecular H-bonding interaction [O28–H··N12 (2.901(2) Å, 169.0°)] building pairs of molecules.

In the crystal, the aforementioned pairs of molecules are further associated by rather strong inter-molecular H-bonds building zig-zag 1D chains [O1–H··O24 (2.700(2) Å, 153.2°) and O21–H··O4 (2.654(2) Å, 152.6°)] (Fig. 4).

Adjacent chains connect to each other by additional H-bonds (see Table S2.3) leading to corrugated ribbons. Finally, hydrophobic interactions connect close ribbons to accomplish the 3D architecture of the crystal.

3.1.3. Crystal structure of the ligand L8

The crystal of ligand L8 crystallizes in the triclinic system, space group P-1. The asymmetric unit consists of just one organic molecule (Fig. 5).

One of the hydroxyl-methyl arms in L8 is delocalized in three different positions [O27A 0.393(12), O27B 0.325(14), O27C 0.283(6)].

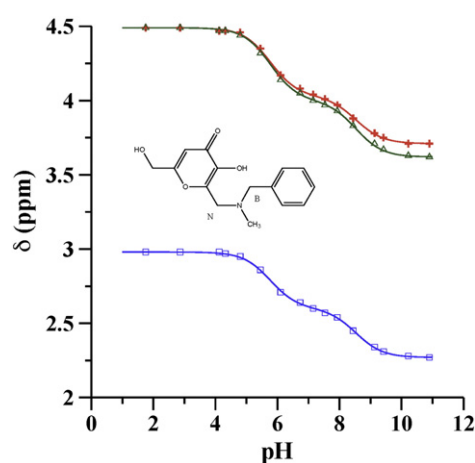


Fig. 8. Chemical shifts of CH₃ (blue squares), CH₂(B) (green triangles) and CH₂(K) (red crosses) of L7 ligand as a function of pH.

Table 2

Chemical shifts of H3, CH₂(K), CH₂(B) and CH₃ protons in the species LH₂⁺, LH and L⁻ of ligand L7, calculated with the HyperNMR program [20].

Species	H3	CH ₂ (K)	CH ₂ (B)	CH ₃
LH ₂ ⁺	6.51	4.49	4.49	2.98
LH	6.41	4.03	4.00	2.60
L ⁻	6.35	3.71	3.72	2.27

Table 3

Chemical shifts of in the species LH₃⁺, LH₂, LH⁻ and L²⁻ of ligands L4 and L5, calculated with the HyperNMR program [20].

Species	L4			L5		
	H3	CH ₂ (N)	CH ₃	H3	CH ₂ (N)	CH(Bn)
LH ₃ ⁺	6.57	4.61	3.11	6.50	4.65	4.61
LH ₂	6.49	3.87	2.55	6.41	3.98	3.92
LH ⁻	6.39	3.93	2.58	6.32	3.95	3.90
L ²⁻	6.39	3.76	2.31	6.29	3.90	3.73

The mean planes of the two kojic moieties define a dihedral angle of 85.02°. This value, and therefore the orientation of the kojic moieties within the organic molecule, is similar to that described for a related bis-kojic derivatives of ortho-vanillin [9]. In accordance to the above-described L6 and L7 ligands, in L8 can also be observed in the corresponding intra-molecular interactions that involve the OH phenol-like group and the O keto-kojic group [O26–H··O25 (2.774(2) Å, 111.63°) and O36–H··O35 (2.756(2) Å, 112.35°)].

The crystal packing of L8 resembles to that of compound L7. Thus, zig-zag 1D chains are built by symmetry related molecules kinked by inter-molecular H-bonding interactions [O(26)–H··O25 (2.653(2) Å, 147.5°) and O36–H··O35 (2.754(2) Å, 154.6°)]. Adjacent chains are further connected by H-bonds (see Table S3.3) leading to corrugated ribbons. Again, the 3D framework is reached by hydrophobic interactions between neighboring ribbons.

3.2. Protonation equilibria

The protonation equilibria of the five ligands have been studied by potentiometry, UV spectrophotometry and ¹H NMR spectroscopy. The protonation constants evaluated from the potentiometric titration curves at 25 °C and 0.1 M ionic strength for the five ligands are reported in Table 1.

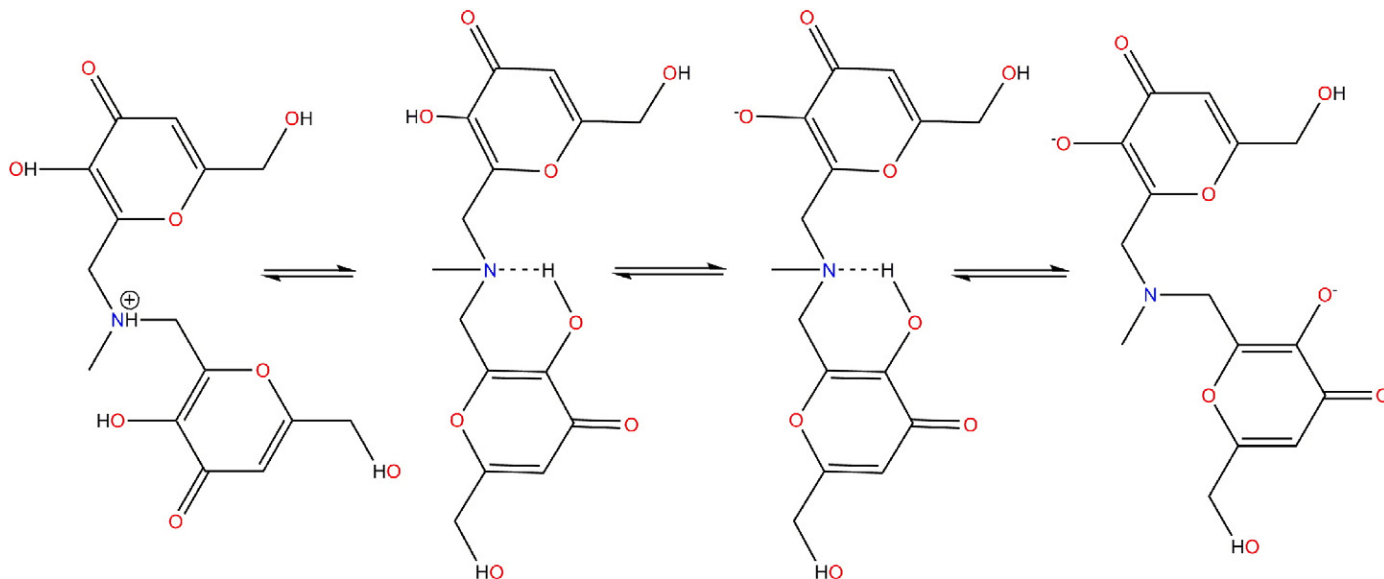
Table 4

Complex formation constants of the five ligands with Fe^{III} at 25 °C, 0.1 M KCl ionic strength, obtained from potentiometric–spectrophotometric data using the Hyperquad program [13]. Charges are omitted for simplicity.

	L4	L5	L6	L7	L8
FeLH ₃	–	–	25.25(3)	–	–
FeLH ₂	22.21(3)	21.9(2)	–	–	–
FeLH	–	–	–	–	18.4(3)
Fe ₂ L ₂	–	–	–	–	41.11(4)
Fe ₂ L ₂ H ₋₁	–	–	–	–	38.97(2)
Fe ₂ L ₃ H ₄	69.1(1)	–	70.3(3)	–	–
Fe ₂ L ₃ H ₃	66.10(4)	67.2(2)	66.2(1)	–	–
Fe ₂ L ₃ H ₂	61.6(2)	64.1(2)	61.2(2)	–	–
Fe ₂ L ₃ H	56.19(1)	59.9(1)	–	–	–
Fe ₂ L ₃	49.75(1)	53.5(1)	49.4(2)	–	55.08(4)
FeL ₂ H ₂	–	–	–	33.0(1)	–
FeL ₂ H	–	–	–	28.2(2)	–
FeL ₂	–	–	–	22.6(2)	–
FeL ₂ H ₋₁	–	–	–	15.7(1)	–
FeL ₃	–	–	–	27.1(1)	–
pFe	18.1	19.3	17.7	16.7	20.0

The ligands L4 and L5 are characterized by three protonation constants, corresponding to the two kojic phenolates and to the nitrogen atom in the linker; L6 by four protonation constants relative to the two kojic units and to the two nitrogen atoms in the piperazine ring; L7 by two protonation constants attributable to the kojic phenolate and the nitrogen atom; L8 by the two protonation constants relative to the two kojic phenolates. The parent molecule kojic acid is characterized by a logK value of 7.70, and the protonation constant of a nitrogen atom in a tertiary amine can be roughly estimated from literature data that range from a value of logK = 8.05 for triethanolamine to 10.70 for triethylamine. As previously reported [7], the L⁻ and LH species of kojic acid are characterized by UV bands at 315 nm (ε = 5900 M⁻¹ cm⁻¹) and 270 nm (ε = 8700 M⁻¹ cm⁻¹), respectively, with sharp isosbestic points at 242 nm and 290 nm.

In the following the protonation sequences of the five ligands, based on the spectrophotometric and ¹H NMR results, are proposed. This discussion starts with the simpler L7 compound, presenting only a kojic phenol group and a protonable nitrogen atom on the linker. Analysis of Fig. 6 (spectra a), in which the spectra collected during the potentiometric titration are presented, shows the band of the fully protonated form LH₂⁺ quite similar to that of the protonated species LH of kojic acid, differing only in the wavelength of the maximum, now shifted from 270 to 276 nm (ε = 8850 M⁻¹ cm⁻¹). The intensity of this

**Scheme 3.** Deprotonation sequence of ligand L4.

band decreases at about one half of its height during the first deprotonation (blue spectra), with the contemporary appearance of a new band at 322 nm, with sharp isosbestic points at 242 nm and 290 nm. During the second deprotonation (red curves) a further decrease in the intensity of the band at 276 nm and an increase in that at 322 nm take place. The band at 322 nm too is shifted to higher wavelengths and its ϵ value at the maximum is slightly higher than that of the corresponding band of fully deprotonated kojic acid. The trends of the peak intensity after decomposition of the spectra in the Gaussian band-components [19], overlapping the speciation plot, are clearly visible in Fig. 7.

A similar trend is presented by the chemical shifts of protons H3, CH₂(K), and CH₂(B) and CH₃ reported in Fig. 8. All these chemical shifts present an upfield shift during the two deprotonations, more marked for the three proton groups proximal to the nitrogen atom.

The chemical shifts of all the kind of protons in the species LH₂⁺, LH and L⁻, calculated with the HyperNMR program [20], are reported in Table 2.

The variations of both UV bands and chemical shifts, about of the same order of magnitude during the first and the second deprotonation, could lead to the hypothesis of a micro-dissociation scheme, in which the first proton is lost in comparable measure both by the nitrogen atom and by the phenolic group. The logK₂ value (6.02) corresponding to the first deprotonation step, ~1.7 units lower than that of kojic acid (and much lower than that of a tertiary amine nitrogen atom), implies a particular stabilization of the monoprotinated species such as the formation of a hydrogen bond between the phenolate O⁻ and the charged NH⁺ nitrogen, or between the phenolic group and the deprotonated nitrogen. Actually, whether the proton is lost by phenolic group or by nitrogen atom, the remaining proton is equally shared in a hydrogen bonding between these groups. Such a situation may well explain the observed experimental trends in which all the UV and NMR signals feel in an equal effect on both deprotonation steps.

Ligands L4 and L5 were characterized by the UV spectra with a maximum at about 275 nm for the fully protonated species, with ϵ values almost double with respect to those of kojic acid and ligand L7; during the first deprotonation step, this band slightly decreased in both ligands, with the appearance of a new band at about 328 nm; in the following steps a more marked decrease of the 275 nm band and an increase of the 328 nm band were observed.

Characteristic variations of the chemical shifts of the H3, CH₂(N), and CH₃ protons in L4, and H3, CH₂(N), and CH(Bn) protons in L5 are observed (Table 3), which allow to propose a sequence in the deprotonations of these ligands similar to that described above for L7. Hence, the first deprotonation leads to a neutral species in which a proton is shared through hydrogen bonding between the nitrogen atom and one of the two kojic phenol groups, inducing the strong upfield shift of the groups neighboring to the nitrogen atom, and that of H3 in the kojic ring. The second deprotonation, taking place on the kojic moiety not involved in the hydrogen bonding, is characterized both by a strong spectral variation of the UV bands related to the kojic moiety, and by an upfield shift of the NMR signals of the H3 proton, while those of the CH₂(N), CH₃ and CH(Bn) protons remain unaffected; in the last step, mainly in L4, a further upfield shift is experienced by hydrogen atoms neighbor to nitrogen for the loss of the shared proton, and a further strong spectral variation of the UV bands. This sequence is briefly sketched in Scheme 3.

Concerning the ligand L6 containing the piperazine ring on the linker, it is characterized by four protonation constants, logK₁ = 8.52, logK₂ = 7.81, logK₃ = 5.49, and logK₄ = 1.97. Presumably the general mechanism of deprotonation could be similar to that observed for L4 and L5, with the involvement of a further basic nitrogen atom. The low L6 water solubility avoided the acquisition of reliable NMR spectra. Furthermore, the small differences between the protonation constants lead to a continuous variation with pH of the UV absorbance bands, without any clear inflection. All these facts prevented to speculate upon the deprotonation mechanism.

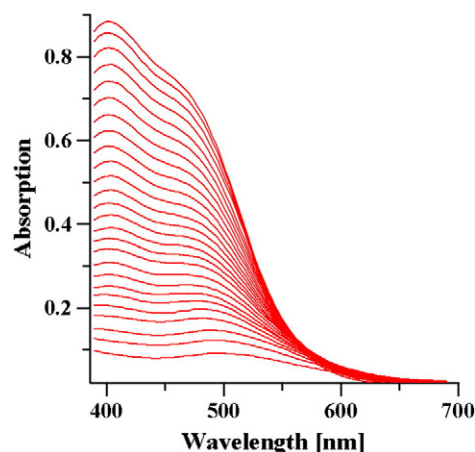


Fig. 9. Spectra collected in pH range 0.8–2.4, from solutions containing L4 = 3.44×10^{-4} M and Fe^{III} = 1.72×10^{-4} M, using 1 cm path length.

Ligand L8 is characterized by two protonation constants almost equal to those of L1, and a trend of UV spectra and NMR chemical shifts similar to that previously reported for L1 ligand was observed.

3.3. Iron complexes

The complex formation equilibria of all the five ligands with Fe^{III} have been studied by combined potentiometric–spectrophotometric techniques. In fact, being Fe^{III} almost completely complexed when

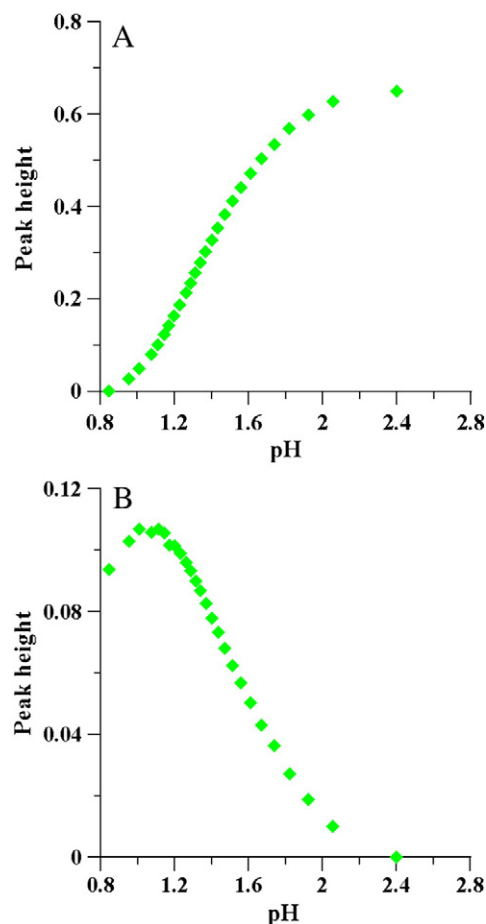


Fig. 10. Trend of the band absorbances at 468 nm (A) and 545 nm (B) reported as a function of pH, after decomposition of the spectra in Fig. 9.

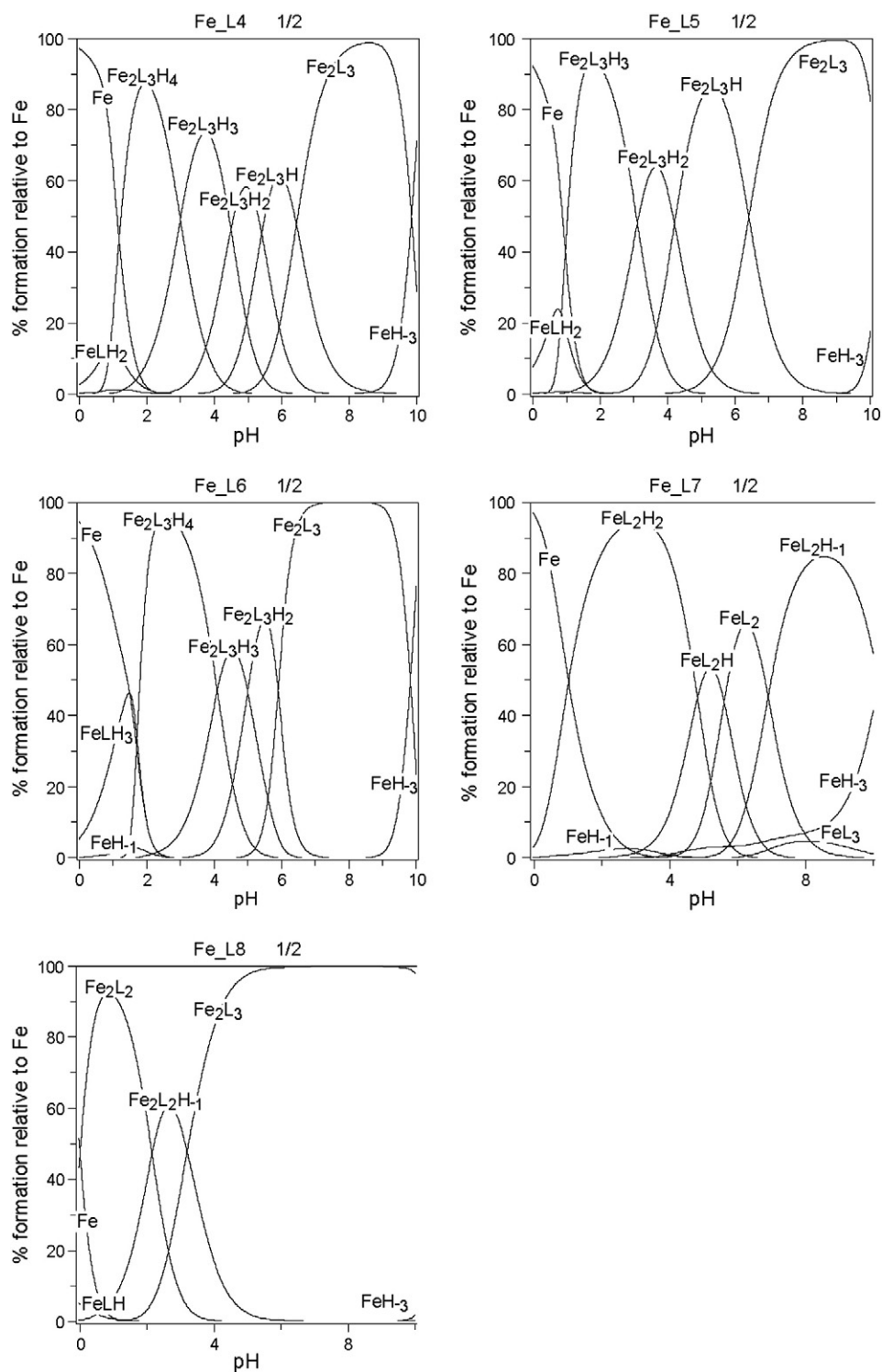


Fig. 11. Speciation plots calculated on the basis of stability constants reported in Table 4, using a ligand concentration 1×10^{-3} M and Fe^{III} concentration 5×10^{-4} M.

mixing reagents before the base potentiometric titrations, the estimation of reliable complex formation constants from potentiometric data alone was prevented. Therefore the complex formation equilibria have been studied both in strong acidic solutions (pH 0–2) on sets of solutions at increasing concentrations of HCl until the disappearance of the bands of complexed iron, and in the pH range 2–10. Simultaneous fitting of potentiometric and spectrophotometric data allowed obtaining the stability constants for the complexes of ligands L4–L8 with Fe^{III} , reported in Table 4.

The three ligands L4, L5, and L6 show a similar behavior; the visible spectra collected in strong acidic solutions at different metal/ligand ratios (1/1, 1/2, 1/3) display the 1:1 complex which at increasing pH soon disappears giving a $\text{Fe}_2\text{L}_3\text{H}_x$ complex stable in the 2–4 pH range. Actually, the shape of the spectra in this pH range is similar for all the three solutions at different metal/ligand ratios, and this is indicative that a unique species is formed. The ratios of the absorbance values in the three solutions clearly indicate the formation of a Fe_2L_3 complex. This has been confirmed by a Job plot performed at pH 2.9, which

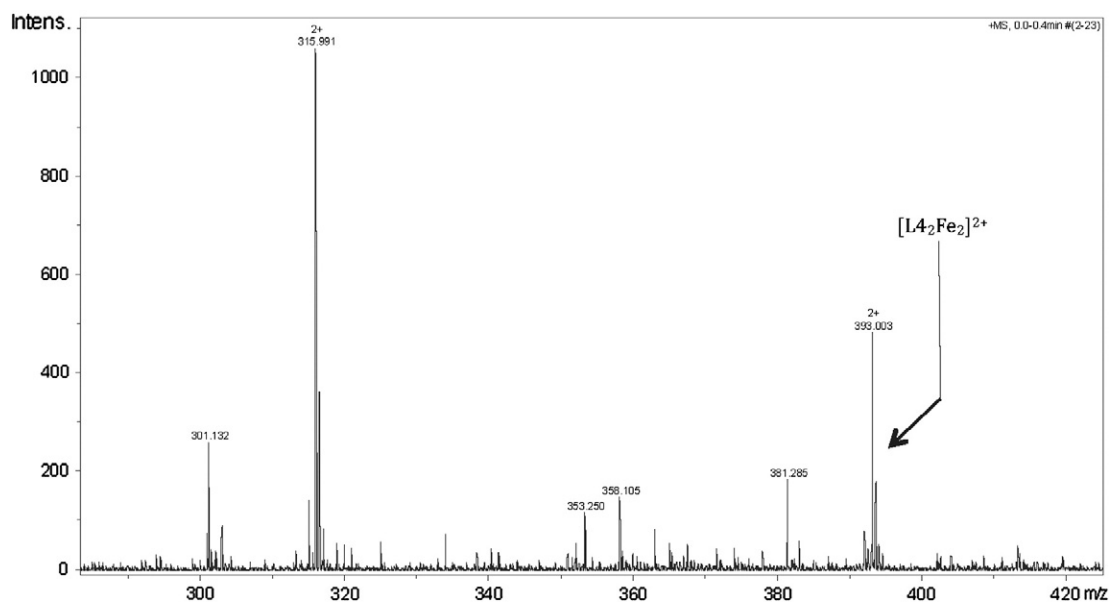


Fig. 12. ESI-MS spectra of the system L4-Fe^{III} in a ratio 1:10 at pH 7.

results in two straight lines intersecting at the ligand mole fraction 0.6. The spectra collected in acidic solutions for the 1:2 ligand/metal molar ratios for ligand L4 are reported in Fig. 9 as an example.

The spectra were decomposed in four Gaussian bands, with the program Specpeak [19]. The absorption of the bands at 468 nm and 545 nm are reported as a function of pH in Fig. 10.

The speciation plots shown in Fig. 11, calculated on the basis of stability constants reported in Table 4, allow some considerations: at very acidic pH (~1) a FeL₂ complex with the two ligands L4 and L5 is formed, in which presumably Fe^{III} is coordinated by the two oxygen atoms of a kojic unit, being the nitrogen atom and the second kojic unit till protonated. At increasing pH a Fe₂L₃H₃ complex appears, in which the two iron atoms are joined by the three ligands, each bonding the two metal ions through its kojic moieties; the complex Fe₂L₃H₄ formed only by the ligand L4 is presumably an intermediate in which two ligands join the two metal ions, and the third ligand binds only one iron atom with a kojic unit, the second one till protonated. Further pH increase induces progressive deprotonations with pK's ~ 4.5, 5.4 and 6.4 for L4 and 3.1, 4.2 and 6.4 for L5. These deprotonations can be reasonably attributed to the loss of protons from the nitrogen atoms in the linker.

A similar behavior is presented by L6, in which a FeLH₃ complex is initially formed, with iron coordinated by a kojic unit, the second kojic unit and the two piperazine nitrogen till protonated. Subsequently a Fe₂L₃H₄ complex is formed, in which the two iron atoms are bridged by the three ligands through both kojic units, with four of the six piperazine nitrogen atoms till protonated. Afterwards, the first two protons are lost with pK values 4.1 and 5.0, and the two last with the same pK 5.9. After several attempts to crystallize the compound Fe₂(L6)₃ a red parallelepiped crystal was obtained and read with Synchrotron radiation but the collected data only allowed seeing a rough model of the complex (See Supplementary Information).

Ligand L7, which does not contain a second kojic unit, forms FeL₂H_x and FeL₃ complexes, similarly to kojic acid. The FeL₂H₂ starting complex, protonated on the nitrogen atoms of both ligands, loses these protons and a third one, presumably from a coordinated water molecule at pK's 4.8, 5.6 and 6.9.

As far as the ligand L8¹ is concerned, its complexation mechanism starts with the formation of a FeLH complex at extremely low pH (0–1)

and it was evidenced only by spectral analysis. Already at these low pH values a Fe₂L₂ complex is formed with the two iron atoms joined by the two ligands. This complex is further stabilized by the loss at pH 2.1 of a proton from a coordinated water molecule, presumably a μ water joining the two iron atoms. At pH ≈ 4 a Fe₂L₃ complex is formed in which each iron atom is completely surrounded by six oxygen atoms from three kojic units.

The ESI-MS spectra, collected at pH ~7, with a 10:1 metal excess, allows revealing further complexes not lighted by the other solution equilibrium techniques. The ESI-MS spectrum of Fe^{III} complexes with L4 is illustrated in Fig. 12. The signal at *m/z* 393.004 reveals a [L₄₂Fe₂]²⁺ complex formation. The peak at *m/z* 315.991 corresponds to [L₄₂Fe₂]²⁺ complex without one methylene-kojic acid molecule. Formation of this complex is probably due to cleavage of the N–C bond during ionization of the [L₄₂Fe₂]²⁺ complex. The signal corresponding to free ligand is not present.

The ESI-MS spectrum in Fig. 13 displays the L5 complex formation. The main peaks appear at *m/z* 392.026, *m/z* 469.040 and *m/z* 478.045. The peak at *m/z* 469.040 corresponds to complex [L₅₂Fe₂]²⁺, while peak at *m/z* 478.045 represents its hydrated form [L₅₂Fe₂]²⁺. Such type of complex is stable even without one methylene kojic acid molecule, since the peak at *m/z* 392.026 is very intense. The peak corresponding to the free ligand is not present.

MS/MS fragmentation of the complex corresponding to signal at *m/z* 392.025 (Fig. 14) results in loss of another methylene-kojic. Signal at *m/z* 315.014 agrees with stoichiometry of [L₅₂Fe₂]²⁺ complex without two methylene kojic acid molecules.

The representative ESI-MS spectrum of Fe^{III} complexes with L6 is presented in Fig. 15. The high intensity of the peak at *m/z* 448.052 corresponds to the [L₆₂Fe₂]²⁺ complex, while the low intensity peak at *m/z* 457.053 represents [L₆₂Fe₂ + H₂O]²⁺ complex.

4. Conclusions

Five new ligands have been synthesized, structurally characterized and their protonation scheme has been explained using the information of UV and ¹H NMR spectra. For all the ligands containing two kojic units, the complex formation equilibria with Fe^{III} allowed concluding about the formation of variously protonated 2:3 Fe:L complex as the major species in the whole pH range; the unprotonated Fe₂L₃ complex is the unique species at pH 7.4 (see speciation plots in Fig. 11). Ligand L7, containing only a kojic unit, forms FeL₂H_x

¹ L8, differently from L4–L7 complexes, does not contain nitrogen atoms, and it is analogous to the previously studied L1 ligand [7].

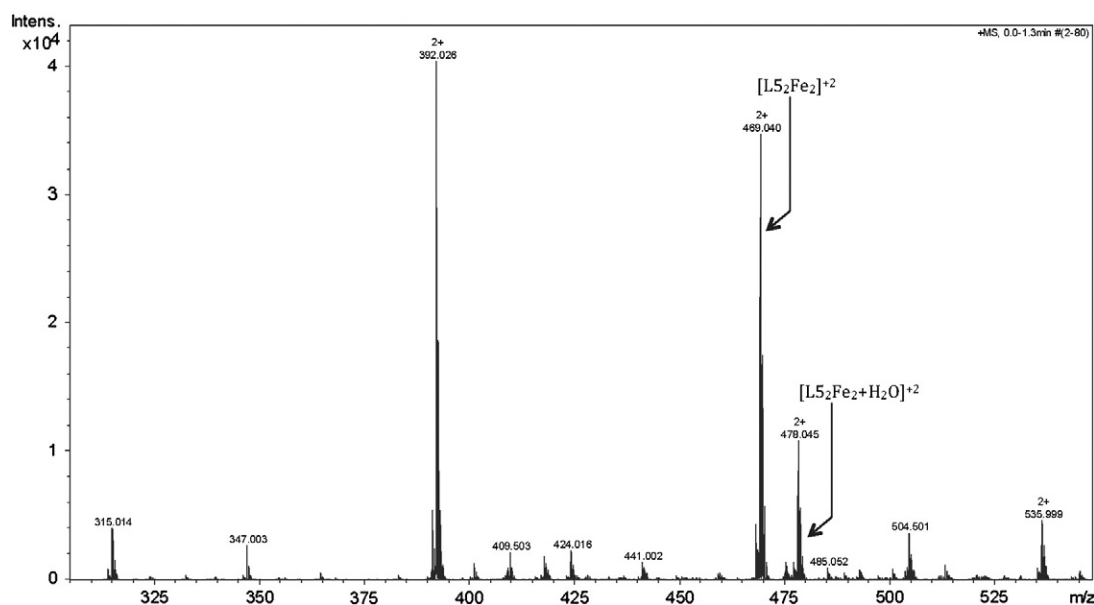


Fig. 13. ESI-MS spectra of the system L5-Fe^{III} in a ratio 1:10 at pH 7.

complexes and, in a lower amount, a FeL₃ complex. The prevailing species at pH 7.4 is FeL₂H₋₁, stabilized by the deprotonation of a coordinated water molecule.

The pFe values reported in Table 4 can be used to evaluate and to compare the chelating ability of the various ligands. These data give evidence of a strong chelating ability of L8 ligand. The remaining ligands L4–L6, containing nitrogen atoms in the linker, show a minor chelating efficiency, pFe ranging from 19.3 for L5 to 17.7 for L6. Interaction of iron with L7 ligand, having only a coordinating kojic unit, is characterized by a pFe value 16.7, ca. 3 units higher than that of simple kojic acid. This significant difference should depend on two facts: the stabilization due to the loss of a proton from a coordinated water molecule, and to a kind of a hydrophobic cage formed by the groups not directly implied in coordination of the metal ion. According to the recent work of Evans [21], L8 ligand, anionic at physiological pH and characterized by a pFe of 20.0, and perhaps L5, partially in the anionic form LH⁻¹ at physiological pH and with pFe = 19.3, should be able to mobilize Fe^{III} from transferrin.

The excellent chelating properties recommend further toxicological and pharmacological research on these new promising ligands.

Acknowledgments

GC and JIL acknowledge Regione Sardegna for the financial support CRP-27564 to the project “Integrated approach in the design of chelators for the treatment of metal overload diseases”. MCA is grateful to RAS for the program Master and Back – Percorsi di rientro, PRR-MAB-A2011-19107. MAS acknowledges FCT for financial support, project PEst-OE/QUI/UI0100/2011.

Appendix A. Supplementary data

Supplementary data to this article can be found online at <http://dx.doi.org/10.1016/j.jinorgbio.2013.06.009>.

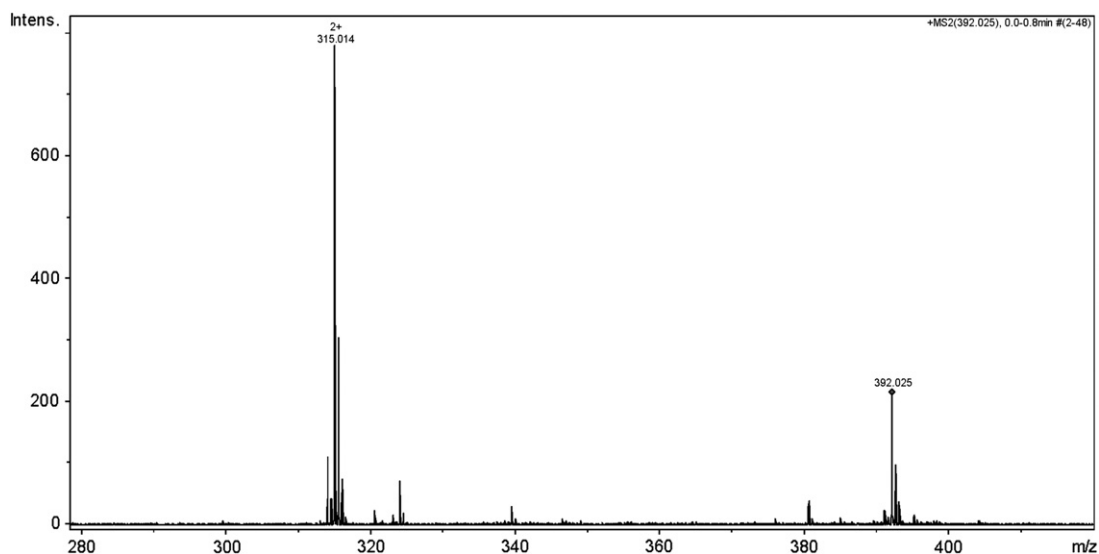


Fig. 14. CAD spectrum of peak at *m/z* 392.025 in Fig. 13.

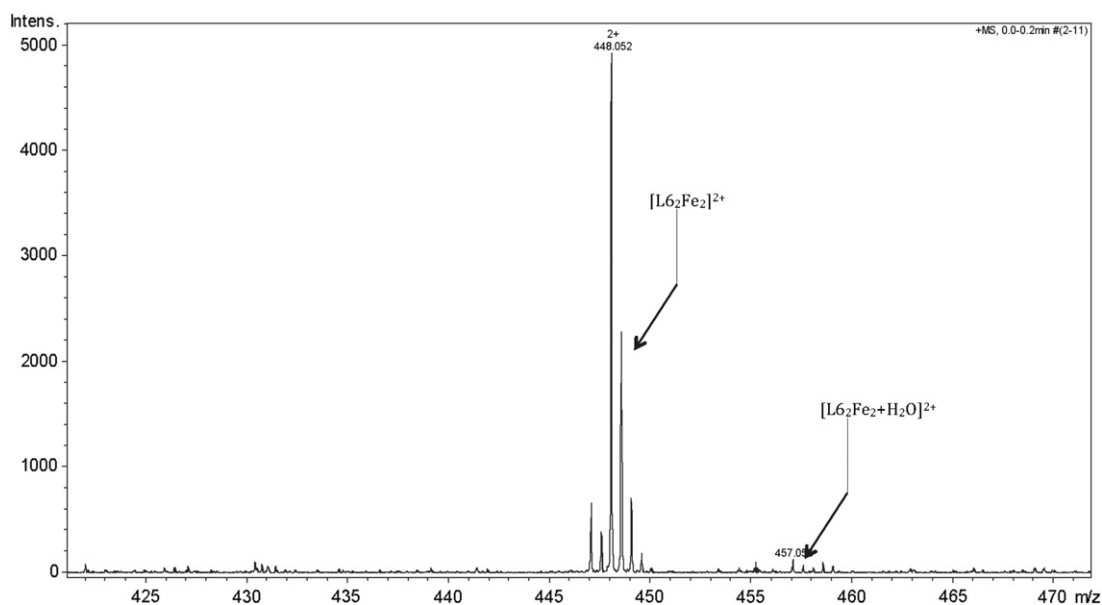


Fig. 15. ESI-MS spectra of the system L6-Fe^{III} in a ratio 1:10 at pH 7.

References

- [1] G. Crisponi, M. Remelli, *Coord. Chem. Rev.* 252 (2008) 1225–1240.
- [2] Y. Ma, T. Zhou, X. Kong, R.C. Hider, *Curr. Med. Chem.* 19 (2012) 2816–2827.
- [3] G. Crisponi, V.M. Nurchi, V. Bertolasi, M. Remelli, G. Faa, *Coord. Chem. Rev.* 256 (2012) 89–104.
- [4] M.A. Santos, S.M. Marques, S. Chaves, *Coord. Chem. Rev.* 256 (2012) 240–259.
- [5] G. Crisponi, V.M. Nurchi, G. Faa, M. Remelli, *Monatsh. Chem.* 142 (2011) 331–340.
- [6] G. Crisponi, A. Dean, V. Di Marco, J.I. Lachowicz, V.M. Nurchi, M. Remelli, A. Tapparo, *Anal. Bioanal. Chem.* 405 (2013) 585–601.
- [7] V.M. Nurchi, G. Crisponi, J.I. Lachowicz, S. Murgia, T. Pivetta, M. Remelli, A. Rescigno, J. Nicolás-Gutiérrez, J.M. González-Pérez, A. Domínguez-Martín, A. Castiñeiras, Z. Szewczuk, *J. Inorg. Biochem.* 104 (2010) 560–569.
- [8] R.C. Fox, P.D. Taylor, *Bioorg. Med. Chem. Lett.* 8 (1998) 443–446.
- [9] V.M. Nurchi, J.I. Lachowicz, G. Crisponi, S. Murgia, M. Arca, A. Pintus, P. Gans, J. Niclos-Gutiérrez, A. Domínguez-Martín, A. Castiñeiras, M. Remelli, Z. Szewczuk, T. Lis, *Dalton Trans.* 40 (2011) 5984–5998.
- [10] V.M. Nurchi, G. Crisponi, T. Pivetta, M. Donatoni, M. Remelli, *J. Inorg. Biochem.* 102 (2008) 684–692.
- [11] V.M. Nurchi, G. Crisponi, M. Crespo-Alonso, J.I. Lachowicz, Z. Szewczuk, G.J.S. Cooper, *Dalton Trans.* 42 (2013) 6161–6170.
- [12] H.N. Barham, G.N. Reed, *J. Am. Chem. Soc.* 60 (1938) 1541–1545.
- [13] P. Gans, A. Sabatini, A. Vacca, *Talanta* 43 (1996) 1739–1753.
- [14] Bruker, APEX2 Software, Bruker AXS Inc., Madison, Wisconsin, USA, 2010. (v2010.3-0).
- [15] G.M. Sheldrick, SADABS, Program for Empirical Absorption Correction of Area Detector Data, University of Gottingen, Germany, 2009.
- [16] G.M. Sheldrick, *Acta Crystallogr. Sect. A* 64 (2007) 112–122.
- [17] A.L. Spek, Utrecht University, Utrecht, The Netherlands, 2010.
- [18] C.F. Macrae, I.J. Bruno, J.A. Chisholm, P.R. Edgington, P. McCabe, E. Pidcock, L. Rodriguez-Monge, R. Taylor, J. Van De Streek, P.A. Wood, *J. Appl. Crystallogr.* 41 (2008) 466–470.
- [19] M.C. Aragoni, M. Arca, G. Crisponi, V.M. Nurchi, *Anal. Chim. Acta* 316 (1995) 195–204.
- [20] C. Frassinetti, L. Alderighi, P. Gans, A. Sabatini, A. Vacca, S. Ghelli, *Anal. Bioanal. Chem.* 376 (2003) 1041–1052.
- [21] R.W. Evans, X. Kong, R.C. Hider, *Biochim. Biophys. Acta* 1820 (2012) 282–290.